ACS OMEGA

http://pubs.acs.org/journal/acsodf

Article

Surface Dissociation Effect on Phosphonic Acid Self-Assembled Monolayer Formation on ZnO Nanowires

Kentaro Nakamura, Tsunaki Takahashi,* Takuro Hosomi, Yu Yamaguchi, Wataru Tanaka, Jiangyang Liu, Masaki Kanai, Kazuki Nagashima, and Takeshi Yanagida*

Cite This: *ACS Omega* 2022, 7, 1462−1467

Read Online

ACCESS | Metrics & More | Article Recommendations | Supporting Information

ABSTRACT: Understanding the formation process of self-assembled monolayers (SAMs) of organophosphonic acids on ZnO surfaces is essential to designing their various applications, including solar cells, heterogeneous catalysts, and molecular sensors. Here, we report the significant effect of surface dissociation on SAM formation of organophosphonic acids on single-crystalline ZnO nanowire surfaces using infrared spectroscopy. When employing the most conventional solvent-methanol (relative permittivity ε_r = 32.6), the production of undesired byproducts (layered zinc compounds) on the surface was identified by infrared spectral data and microscopy. On the other hand, a well-defined SAM structure with a tridentate coordination of phosphonic acids on the surface was confirmed when employing toluene (ε_r = 2.379) or *tert*-butyl alcohol (ε_r = 11.22−11.50). The observation of layered zinc compounds as byproducts highlights that the degree of Zn^{2+} dissociation from the ZnO solid surface into a solvent significantly affects the surface coordination of phosphonic acids during the SAM formation process. Although the ZnO nanowire surface (*m*-plane) is hydrophilic, the present results suggest that a weaker solvent polarity is preferred to form well-defined phosphonic acid SAMs on ZnO nanowire surfaces without detrimental surface byproducts.

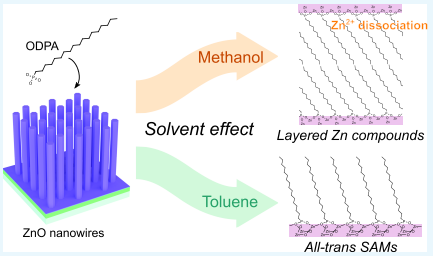

INTRODUCTION

Molecular surface modification on metal oxide nanostructures has shown great promise to tailor their surface functionalities for various applications, including heterogeneous catalysts[1,2] and molecular sensors.[3,4] One of the promising molecular surface modifications is applying self-assembled monolayers (SAMs) on metal oxide surfaces.[5−7] Various SAMs have been successfully introduced onto surfaces of various metal oxide nanostructures, including thin films, nanowires, nanoparticles, and others.[5,8−10] For example, SAMs were applied onto ITO substrates to modulate the work function.[11,12] Among various head groups of SAMs, a phosphonic acid has particularly attracted the significant attention of many researchers[13−18] because phosphonic acids provide a more robust modification layer when compared to those formed from carboxylic acids, especially after annealing to maximize the number of P−O bonds.[19−22] For example, interesting applications using phosphonic acid SAMs on ZnO surfaces have been successfully demonstrated[8−10,13−15,21−23] since ZnO is one of the most popular metal oxide materials.[24−26] Zhang *et al.* have reported the formation of phosphonic acid SAMs on ZnO surfaces.[14] Lim *et al.* demonstrated the long-term stability and high sensing selectivity with phosphonic acid SAM modified ZnO nanowire sensors.[27] Despite these successes of phosphonic acid SAMs on ZnO nanostructures, the nature of the formation process is still complex and affected by many experimental parameters, including temperature,[28,29] concentration and modification time,[30] solid surface and material,[18,31,32] and solvent.[20,21] Solvent selection for the SAM formation process is especially important because the solvent must dissolve the SAM molecules.[33] Literature survey for phosphonic acid SAMs on ZnO surfaces reveals that the major solvents for these SAM formation processes are alcohols, including methanol, ethanol, and others.[29,34−37] Although Chen *et al.* have reported the solvent effect on the phosphonic acid SAM formation process on ITO substrates,[38] such solvent effects on phosphonic acid SAM formation processes on ZnO nanostructures have not been studied. Here, we report the significant impact of surface dissociation on SAM formation of organophosphonic acids on single-crystalline ZnO nanowire surfaces using infrared spectroscopy. We found that the degree of Zn^{2+} dissociation from the ZnO solid surface into a solvent strongly affects the surface coordination of phosphonic acids during the SAM formation process.

Received: November 4, 2021
Accepted: December 14, 2021
Published: December 27, 2021

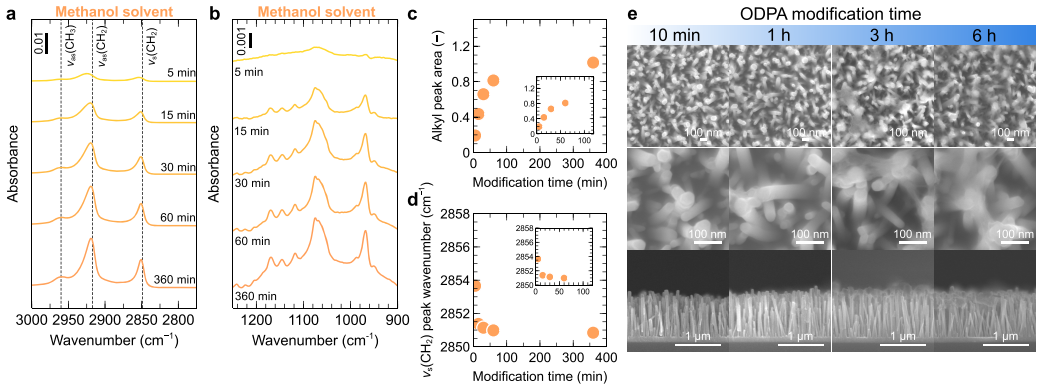

Figure 1. FT-IR spectra of ODPA on ZnO nanowires in the (a) alkyl or (b) phosphonic acid region for an ODPA concentration of 0.1 mM in methanol solvent. ODPA modification time dependence of (c) alkyl peak area and (d) wavenumber of CH_2 symmetric stretch vibration ($\nu_s(CH_2)$). Inset figures show enlarged characteristics at an early stage of SAM formation. (e) FESEM images of ODPA modified ZnO nanowires using methanol solvent. The ODPA concentration was 0.1 mM for all samples.

RESULTS AND DISCUSSION

Figure 1a,b shows the time-series data of FT-IR during SAM formation processes of octadecylphosphonic acid (ODPA) on ZnO nanowires in methanol solvent. The concentration of ODPA is 0.1 mM. The details of ZnO nanowire growth processes can be seen in Methods. The analyzed data (the alkyl peak area and the wavenumber of CH_2 symmetric stretch vibration-$\nu_s(CH_2)$) are shown in Figure 1c,d. Clearly, the IR-absorbance of SAMs in Figure 1a,b tends to be stronger with increasing surface modification time, as also seen in Figure 1c. As seen in Figure 1a,d, the wavenumber of $\nu_s(CH_2)$ tends to decrease from 2853.7 down to 2850.8 cm^{-1}. This trend is well known as the alkyl chain conformation change from gauche to all-trans geometry with increasing SAM surface density.[39,40] Although the interpretation of absorption bands of alkyl chains (2800−3000 cm^{-1}) is straightforward, the absorption bands for phosphonic acids (900−1250 cm^{-1}) exhibit rather complicated spectra, as seen in Figure 1b. Previous studies on IR spectra of phosphonic acid SAMs have reported different identifications on their data.[5,10,13,16,41] For example, the peaks around 900−1050 cm^{-1} were assigned to the P−OH group by comparing the obtained IR peaks of SAMs with the IR peaks of phosphonic acid powder.[5,14,41,42] The peaks around 1040 cm^{-1} were determined to be the stretching modes of PO_3^{2-},[41] which involve P−O and P═O terminations.[41] The peak around 1220 cm^{-1} was reported to be P═O stretching.[29] Although their identifications are rather different in detail, these identifications based on IR peaks of phosphonic acid powder assume the existence of phosphonic acid SAMs on ZnO surfaces without considering surface side reactions. Figure 1e shows the scanning electron microscope (SEM) images of ZnO nanowire surfaces when varying the SAM surface modification time. As clearly seen in the SEM images, some foggy nanostructures on the nanowire surfaces appear with increasing SAM modification time. The foggy nanostructure becomes clear in ODPA modified ZnO nanowires with a SAM modification time of 24 h (Figure S1). Since the emergence of such nanostructures during the SAM formation process is distinct, it is important to identify the structure of the foggy nanostructures.

First, we performed X-ray diffraction (XRD) measurements to identify the structure of foggy nanostructures on ZnO nanowire surfaces, as seen in Figure S2. Unfortunately, conventional XRD measurements could not detect any significant signals for the foggy surface nanostructures, presumably due to the randomness of crystal orientation and the small amount. Here, we consider possible side surface reactions during phosphonic acid SAM formation on ZnO surfaces. One of the plausible surface reactions is the formation of layered zinc phosphonate (Zn-ODP) structures, as illustrated in Figure 2a.[43] Figure 2b shows the comparison

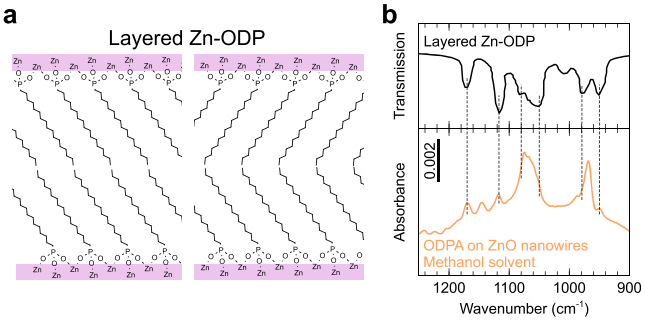

Figure 2. (a) Schematic diagram of the layered Zn-ODP structure. (b) FT-IR spectrum of ODPA on ZnO nanowires in the phosphonic acid region for an ODPA concentration of 0.1 mM for 60 min in methanol solvent. The reported FT-IR spectrum of layered Zn-ODP[43] is also shown.

between the present IR spectrum and the previously reported IR spectrum for the layered Zn-ODP structures.[43] Clearly, there is a good correlation between the two spectra. Especially, the six IR peaks (around 940, 980, 1060,1080, 1120, and 1170 cm^{-1}) are well consistent with such IR peaks of the layered Zn-ODP structures. Note that some peaks in the present samples are not consistent with those of the layered Zn-ODP structures. Thus, based on these results, we conclude that the observed surface nanostructures during phosphonic acid SAM formation on ZnO surfaces are layered Zn-ODP. For well-defined phosphonic acid SAMs on ZnO surfaces, this layered Zn-ODP formation is detrimental. It is noted that the present series of experiments were performed using the most conventional solvent-methanol.[34,35] Next, we solve this undesired side surface reaction issue by considering the reaction mechanism.

To form layered Zn-ODP on ZnO, a dissociation of Zn^{2+} from ZnO nanowire surfaces must be significant; otherwise, simple phosphonic acid SAM formations should occur. Based on this speculation, we change the solvent from relatively polar

https://doi.org/10.1021/acsomega.1c06183
ACS Omega 2022, 7, 1462−1467

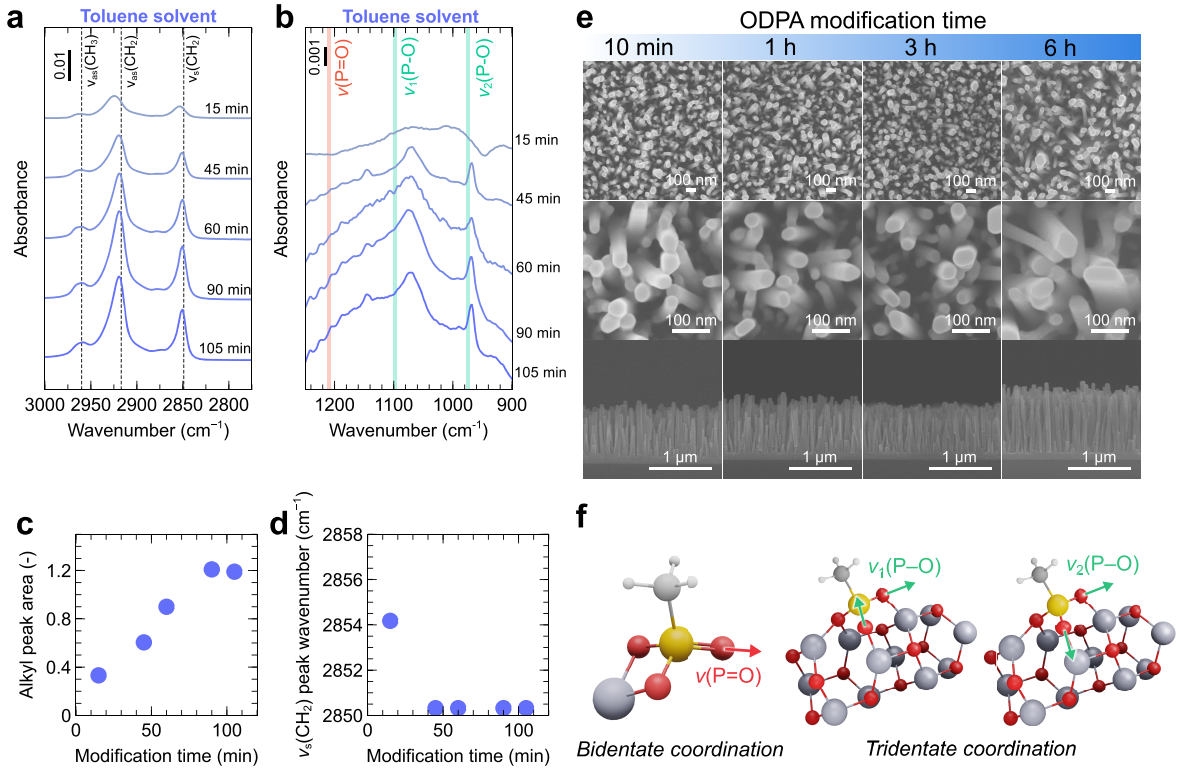

Figure 3. FT-IR spectra of ODPA on ZnO nanowires in the (a) alkyl or (b) phosphonic acid region for an ODPA concentration of 0.1 mM in toluene solvent. ODPA modification time dependence of (c) alkyl peak area and (d) wavenumber of CH_2 symmetric stretch vibration ($\nu_s(CH_2)$). DFT-calculated vibrations of P═O (ν(P═O)) and P−O (ν_1(P−O), ν_2(P−O)) are also indicated. (e) FESEM images of ODPA modified ZnO nanowires using toluene solvent. The ODPA concentration was 0.1 mM for all samples. (f) Optimized structure of bidentate coordination of phosphonic acid on Zn and tridentate coordination on the hexagonal ZnO (10−10) plane calculated by DFT simulations.

methanol (relative permittivity ε_r = 32.6[44]) to non-polar toluene (ε_r = 2.379[44]) to suppress the degree of dissociation of Zn^{2+} from the ZnO nanowire surface. Figure 3a−e shows the results of phosphonic acid SAM formation on ZnO nanowire surfaces when employing toluene as the solvent. There is a significant difference between the two solvents (methanol and toluene) on the FT-IR spectra and SEM images. First, when comparing between Figures 3b and 1b on absorption bands for phosphonic acids (900−1250 cm^{-1}), the spectra of toluene-solvent samples exhibit mainly three peaks (970, 1070, and 1140 cm^{-1}), which are also found in Figure 1b with other peaks from the layered Zn-ODP. Thus, these results highlight that the surface molecular conformation of phosphonic acids is strongly affected by the solvent. As seen in Figure 3c, the SAM formation speed in toluene solvent is slower than that in methanol solvent in Figure 1c. Interestingly, the data of Figure 3d implies that the degree of all-trans geometry is higher for toluene solvent than that for methanol solvent because the wavenumber of $\nu_s(CH_2)$ is lower for toluene solvent. More importantly, SEM observations in Figure 3e do not show any surface nanostructures during the phosphonic acid SAM formation process, which is rather different from the trend in Figure 1e. Therefore, altering the solvent from polar methanol to non-polar toluene significantly suppresses the emergence of surface side reactions and formation of layered Zn-ODP on the ZnO nanowire surface. The proposed strategy of using a non-polar solvent was confirmed by performing experiments using *tert*-butyl alcohol solvent (ε_r = 11.22−11.50[45,46]). Figure S3 shows the FT-IR spectra of ODPA on ZnO nanowires using *tert*-butyl alcohol solvent, which agrees well with that using toluene solvent (Figure 3a−d). Thus, the suppression of side surface reactions was achieved in *tert*-butyl alcohol solvent with weaker polarity than methanol. Finally, we attempt to identify the molecular conformation of phosphonic acids when using toluene by comparing with DFT calculations, as illustrated in Figure 3f. The calculated wavenumbers for a bidentate coordination with P═O and a tridentate coordination without P═O of phosphonic acids on ZnO surfaces are shown in Figure 3b. The comparison between experimental spectra and DFT simulations reveals the existence of a tridentate coordination of phosphonic acids on ZnO surfaces when employing toluene solvent. Thus, these results highlight that phosphonic acid SAM formation on ZnO surfaces requires non-polar solvent-toluene rather than conventional polar solvent-methanol to perform well-defined SAM formation without detrimental surface side reactions with byproducts, although the ZnO nanowire surface is hydrophilic.

CONCLUSIONS

We demonstrate the significant effect of surface dissociation on SAM formation of organophosphonic acids on single-crystalline ZnO nanowire surfaces using infrared spectroscopy. When employing the most conventional solvent-methanol (relative permittivity ε_r = 32.6), the presence of undesired byproducts (layered zinc compounds) on the surface was identified by infrared spectral data and microscopy. On the other hand, a well-defined SAM structure with a tridentate coordination of phosphonic acids on the surface was confirmed when employing toluene (ε_r = 2.379) or *tert*-butyl alcohol (ε_r = 11.22−11.50). The observation of layered zinc compounds as

https://doi.org/10.1021/acsomega.1c06183
ACS Omega 2022, 7, 1462−1467

byproducts highlights that the degree of Zn^{2+} dissociation from the ZnO solid surface into a solvent significantly affects the surface coordination of phosphonic acids during the SAM formation process. Although the ZnO nanowire surface (*m*-plane) is hydrophilic, the present results suggest that a weaker solvent polarity is preferred to form well-defined phosphonic acid SAMs on ZnO nanowire surfaces without detrimental surface byproducts.

METHODS

ZnO Nanowire Growth. Single-crystalline ZnO nanowires were hydrothermally grown on a ZnO seed layer/SiO_2/p-Si substrate. A 5 nm Ti adhesion layer and 100 nm ZnO seed layer were sequentially deposited onto a 100 nm SiO_2/p-type Si substrate by radio frequency (RF) sputtering. Solutions for hydrothermal reactions were mixtures composed of 5 mM zinc nitrate hexahydrate, $Zn(NO_3)_2{\cdot}6H_2O$ (Wako, 99.0%) and 5 mM hexamethylenetetramine (HMTA), $(CH_2)_6N_4$ (Wako, 99.0%). The ZnO-deposited substrate was immersed in the growth solution and kept at 80 °C for 24 h. A ZnO nanowire array was obtained on the substrate after the reaction. After growth, the samples were rinsed with DI water and IPA. Then the ZnO nanowires were annealed for 1 h at 600 °C in atmospheric air to prevent surface degradation.[47]

Modification of Octadecylphosphonic Acid SAMs on ZnO Nanowires. Modification solutions (0.1 mM) were prepared by dissolving octadecylphosphonic acid (ODPA) in methanol or toluene. The annealed ZnO nanowire array was dipped in the solution (10 mL) at room temperature. Then, the samples were washed with methanol or toluene and tetrahydrofuran. After air flow drying, the ODPA modified ZnO nanowire arrays were annealed for 30 min at 150 °C in atmospheric air.

Characterizations. Scanning electron microscope (SEM) images were acquired using a JEOL JSM7610F instrument. The SEM images (Figures 1e and 3e) confirm that the grown ZnO nanowires exhibit hexagonal columnar structures (diameter of ∼100 nm), which indicates that the ZnO nanowires have a single wurtzite structure with the prism (10−10) plane as the main face. Structural characterizations of ZnO nanowires were determined by XRD (PHILIPS, X'Pert MRD 45 kV, 40 mA). The FT-IR spectra of the surface molecules on the ZnO nanowires were recorded at room temperature on a Thermo Fisher Scientific Nicolet iS50 FT-IR spectrometer equipped with a mercury-cadmium-telluride (MCT) detector. 300 scans were accumulated to obtain each spectrum. The test room was purged with dry air. The FT-IR spectrum for bare ZnO was used as the background spectrum for the other measurements. For FT-IR experiments, a double-polished float-zone Si substrate was used for the ZnO nanowire array samples. To analyze the change in the relative amount of alkyl chains, the peak area was calculated by integrating the region from 2800 to 3000 cm^{-1} of the IR absorption spectrum.

Computational Details. We computed the vibrational frequencies of phosphonic acid on ZnO (10−10) surfaces using density functional theory (DFT) to assign the P−O stretching bands. Simplified cluster models with partially fixed coordinations frozen atoms (see Table S1) were employed to consider the adsorbed ZnO (10−10) surface approximately. These models were extracted from a wurtzite ZnO crystal structure with $a = b = 3.25$ Å and $c = 5.2$ Å. The DFT calculations were carried out using the Gaussian 16 program suite Revision A03 with the B3LYP hybrid functional.[48] The obtained harmonic vibrational frequencies were shifted using a scale factor of 0.964[49] to incorporate anharmonic effects effectively.

ASSOCIATED CONTENT

Supporting Information

The Supporting Information is available free of charge at https://pubs.acs.org/doi/10.1021/acsomega.1c06183.

FESEM images of ODPA modified ZnO nanowires using methanol solvent; XRD analyses of bare ZnO nanowires and ODPA modified ZnO nanowires; IR spectra of ODPA modified ZnO nanowires using *tert*-butyl alcohol solvent; optimized molecular geometries of phosphonic acid on ZnO (PDF)

AUTHOR INFORMATION

Corresponding Authors

Tsunaki Takahashi − *Department of Applied Chemistry, Graduate School of Engineering, The University of Tokyo, Tokyo 113-8656, Japan; JST, PRESTO, Kawaguchi, Saitama 332-0012, Japan;* orcid.org/0000-0002-2840-8038; Email: takahashi-t@g.ecc.u-tokyo.ac.jp

Takeshi Yanagida − *Department of Applied Chemistry, Graduate School of Engineering, The University of Tokyo, Tokyo 113-8656, Japan; Institute for Materials Chemistry and Engineering, Kyushu University, Kasuga, Fukuoka 816-8580, Japan;* orcid.org/0000-0003-4837-5701; Email: yanagida@g.ecc.u-tokyo.ac.jp

Authors

Kentaro Nakamura − *Department of Applied Chemistry, Graduate School of Engineering, The University of Tokyo, Tokyo 113-8656, Japan; Institute for Materials Chemistry and Engineering, Kyushu University, Kasuga, Fukuoka 816-8580, Japan*

Takuro Hosomi − *Department of Applied Chemistry, Graduate School of Engineering, The University of Tokyo, Tokyo 113-8656, Japan; JST, PRESTO, Kawaguchi, Saitama 332-0012, Japan;* orcid.org/0000-0002-5649-6696

Yu Yamaguchi − *Department of Applied Chemistry, Graduate School of Engineering, The University of Tokyo, Tokyo 113-8656, Japan*

Wataru Tanaka − *Department of Applied Chemistry, Graduate School of Engineering, The University of Tokyo, Tokyo 113-8656, Japan*

Jiangyang Liu − *Department of Applied Chemistry, Graduate School of Engineering, The University of Tokyo, Tokyo 113-8656, Japan;* orcid.org/0000-0001-5456-7705

Masaki Kanai − *Institute for Materials Chemistry and Engineering, Kyushu University, Kasuga, Fukuoka 816-8580, Japan*

Kazuki Nagashima − *Department of Applied Chemistry, Graduate School of Engineering, The University of Tokyo, Tokyo 113-8656, Japan; JST, PRESTO, Kawaguchi, Saitama 332-0012, Japan;* orcid.org/0000-0003-0180-816X

Complete contact information is available at: https://pubs.acs.org/10.1021/acsomega.1c06183

Notes

The authors declare no competing financial interest.

https://doi.org/10.1021/acsomega.1c06183
ACS Omega 2022, 7, 1462−1467

■ ACKNOWLEDGMENTS

This work was supported by KAKENHI (Grant Numbers: JP20H02208 and JP18H05243). T.T. was supported by JST PREST Grant Number JPMJPR19M6, Japan. T.T., K.N., and T.Y. were supported by JST CREST, Grant Number JPMJCR19I2, Japan. This work was performed under the Cooperative Research Program of the "Network Joint Research Center for Materials and Devices" and the MEXT Project of "Integrated Research Consortium on Chemical Sciences".

■ REFERENCES

(1) Latham, A. H.; Williams, M. E. Controlling Transport and Chemical Functionality of Magnetic Nanoparticles. *Acc. Chem. Res.* **2008**, *41*, 411−420.
(2) Zhang, Q.; Lee, I.; Joo, J. B.; Zaera, F.; Yin, Y. Core-Shell Nanostructured Catalysts. *Acc. Chem. Res.* **2013**, *46*, 1816−1824.
(3) Zheng, G.; Patolsky, F.; Cui, Y.; Wang, W. U.; Lieber, C. M. Multiplexed Electrical Detection of Cancer Markers with Nanowire Sensor Arrays. *Nat. Biotechnol.* **2005**, *23*, 1294−1301.
(4) Feng, L.; Zhu, C.; Yuan, H.; Liu, L.; Lv, F.; Wang, S. Conjugated Polymer Nanoparticles: Preparation, Properties, Functionalization and Biological Applications. *Chem.Soc.Rev.* **2013**, *42*, 6620−6633.
(5) Dembereldorj, U.; Ganbold, E.-O.; Seo, J.-H.; Lee, S. Y.; Yang, S. I.; Joo, S.-W. Conformational Changes of Proteins Adsorbed onto ZnO Nanoparticle Surfaces Investigated by Concentration-Dependent Infrared Spectroscopy. *Vib. Spectrosc.* **2012**, *59*, 23−28.
(6) Marcinko, S.; Fadeev, A. Y. Hydrolytic Stability of Organic Monolayers Supported on TiO_2 and ZrO_2. *Langmuir* **2004**, *20*, 2270−2273.
(7) Hofer, R.; Textor, M.; Spencer, N. D.; Zu, C. Alkyl Phosphate Monolayers , Self-Assembled from Aqueous Solution onto Metal Oxide Surfaces. *Langmuir* **2001**, *17*, 4014−4020.
(8) Kedem, N.; Blumstengel, S.; Henneberger, F.; Cohen, H.; Hodes, G.; Cahen, D. Morphology-, Synthesis- and Doping-Independent Tuning of ZnO Work Function Using Phenylphosphonates. *Phys. Chem. Chem. Phys.* **2014**, *16*, 8310−8319.
(9) Wood, C.; Li, H.; Winget, P.; Bre, J.-L. Binding Modes of Fluorinated Benzylphosphonic Acids on the Polar ZnO Surface and Impact on Work Function. *J. Phys. Chem. C* **2012**, *116*, 19125−19133.
(10) Quiñones, R.; Shoup, D.; Behnke, G.; Peck, C.; Agarwal, S.; Gupta, R. K.; Fagan, J. W.; Mueller, K. T.; Iuliucci, R. J.; Wang, Q. Study of Perfluorophosphonic Acid Surface Modifications on Zinc Oxide Nanoparticles. *Materials* **2017**, *10*, 1−16.
(11) Rittich, J.; Jung, S.; Siekmann, J.; Wuttig, M. Indium-Tin-Oxide (ITO) Work Function Tailoring by Covalently Bound Carboxylic Acid Self-Assembled Monolayers. *Phys. Status Solidi B* **2018**, *255*, 1800075.
(12) Kim, J. S.; Park, J. H.; Lee, J. H.; Jo, J.; Kim, D. Y.; Cho, K. Control of the Electrode Work Function and Active Layer Morphology via Surface Modification of Indium Tin Oxide for High Efficiency Organic Photovoltaics Control of the Electrode Work Function and Active Layer Morphology Organic Photovoltaics. *Appl. Phys. Lett.* **2007**, *91*, 112111.
(13) Braid, J. L.; Koldemir, U.; Sellinger, A.; Collins, R. T.; Furtak, T. E.; Olson, D. C. Conjugated Phosphonic Acid Modified Zinc Oxide Electron Transport Layers for Improved Performance in Organic Solar Cells. *ACS Appl. Mater. Interfaces* **2014**, *6*, 19229−19234.
(14) Zhang, B.; Kong, T.; Xu, W.; Su, R.; Gao, Y.; Cheng, G. Surface Functionalization of Zinc Oxide by Carboxyalkylphosphonic Acid Self-Assembled Monolayers. *Langmuir* **2010**, *26*, 4514−4522.
(15) Ostapenko, A.; Klöffel, T.; Meyer, B.; Witte, G. Formation and Stability of Phenylphosphonic Acid Monolayers on ZnO: Comparison of in Situ and Ex Situ SAM Preparation. *Langmuir* **2016**, *32*, 5029−5037.
(16) Rusu, C. N.; Yates, J. T. Adsorption and Decomposition of Dimethyl Methylphosphonate on TiO_2. *J. Phys. Chem. B* **2000**, *104*, 12292−12298.
(17) Ballesteros-Soberanas, J.; Ellis, L. D.; Medlin, J. W. Effects of Phosphonic Acid Monolayers on the Dehydration Mechanism of Aliphatic Alcohols on TiO_2. *ACS Catal.* **2019**, *9*, 7808−7816.
(18) Ellis, L. D.; Ballesteros-soberanas, J.; Schwartz, D. K.; Medlin, J. W. Effects of Metal Oxide Surface Doping with Phosphonic Acid Monolayers on Alcohol Dehydration Activity and Selectivity. *Appl. Catal. A, Gen.* **2019**, *571*, 102−106.
(19) Bobb-semple, D.; Zeng, L.; Cordova, I.; Bergsman, D. S.; Nordlund, D.; Bent, S. F. Substrate-Dependent Study of Chain Orientation and Order in Alkylphosphonic Acid Self-Assembled Monolayers for ALD Blocking. *Langmuir* **2020**, *36*, 12849−12857.
(20) Lange, I.; Reiter, S.; Kniepert, J.; Piersimoni, F.; Pa∈tzel, M.; Hildebrandt, J.; Brenner, T.; Hecht, S.; Neher, D. Zinc Oxide Modified with Benzylphosphonic Acids as Transparent Electrodes in Regular and Inverted Organic Solar Cell Structures. *Appl. Phys. Lett.* **2015**, *106*, 113302.
(21) Lange, I.; Reiter, S.; Pätzel, M.; Zykov, A.; Nefedov, A.; Hildebrandt, J.; Hecht, S.; Kowarik, S.; Wöll, C.; Heimel, G.; Neher, D. Tuning the Work Function of Polar Zinc Oxide Surfaces Using Modified Phosphonic Acid Self-Assembled Monolayers. *Adv. Funct. Mater.* **2014**, *24*, 7014−7024.
(22) Perkins, C. L. Molecular Anchors for Self-Assembled Monolayers on ZnO: A Direct Comparison of the Thiol and Phosphonic Acid Moieties. *J. Phys. Chem. C* **2009**, *113*, 18276−18286.
(23) Yoshida, H.; Yanagida, T. Phosphonic Acid Modified ZnO Nanowire Sensors: Directing Reaction Pathway of Volatile Carbonyl Compounds. *ACS Appl. Mater. Interfaces* **2020**, *12*, 44265−44272.
(24) Xu, S.; Wang, Z. L. One-Dimensional ZnO Nanostructures: Solution Growth and Functional Properties. *Nano Res.* **2011**, *4*, 1013−1098.
(25) Pourmortazavi, S. M.; Marashianpour, Z.; Karimi, M. S.; Mohammad-Zadeh, M. Electrochemical Synthesis and Characterization of Zinc Carbonate and Zinc Oxide Nanoparticles. *J. Mol. Struct.* **2015**, *1099*, 232−238.
(26) Kanai, M.; Zeng, H.; Mizukami, W.; Shioya, N.; Shimoaka, T. Rational Method of Monitoring Molecular Transformations on Metal-Oxide Nanowire Surfaces. *Nano Lett.* **2019**, *19*, 2443−2449.
(27) Lim, T.; Bong, J.; Mills, E. M.; Kim, S.; Ju, S. Highly Stable Operation of Metal Oxide Nanowire Transistors in Ambient Humidity, Water, Blood, and Oxygen. *ACS Appl. Mater. Interfaces* **2015**, *7*, 16296−16302.
(28) Sang, L.; Knesting, K. M.; Bulusu, A.; Sigdel, A. K.; Giordano, A. J.; Marder, S. R.; Berry, J. J.; Graham, S.; Ginger, D. S.; Pemberton, J. E. Effect of Time and Deposition Method on Quality of Phosphonic Acid Modifier Self-Assembled Monolayers on Indium Zinc Oxide. *Appl. Surf. Sci.* **2016**, *389*, 190−198.
(29) Hotchkiss, P. J.; Malicki, M.; Giordano, A. J.; Armstrong, N. R.; Marder, S. R. Characterization of Phosphonic Acid Binding to Zinc Oxide. *J. Mater. Chem.* **2011**, *21*, 3107−3112.
(30) Bulusu, A.; Paniagua, S. A.; Macleod, B. A.; Sigdel, A. K.; Berry, J. J.; Olson, D. C.; Marder, S. R.; Graham, S. Efficient Modification of Metal Oxide Surfaces with Phosphonic Acids by Spray Coating. *Langmuir* **2013**, *29*, 3935−3942.
(31) Brennan, B. J.; Llansola Portolés, M. J.; Liddell, P. A.; Moore, T. A.; Moore, A. L.; Gust, D. Comparison of Silatrane, Phosphonic Acid, and Carboxylic Acid Functional Groups for Attachment of Porphyrin Sensitizers to TiO_2 in Photoelectrochemical Cells. *Phys. Chem. Chem. Phys.* **2013**, *15*, 16605−16614.
(32) Liu, T.-L.; Bent, S. F. Area-Selective Atomic Layer Deposition on Chemically Similar Materials: Achieving Selectivity on Oxide/Oxide Patterns. *Chem. Mater.* **2021**, *33*, 513−523.
(33) Pellerite, M. J.; Dunbar, T. D.; Boardman, L. D.; Wood, E. J. Effects of Fluorination on Self-Assembled Monolayer Formation from Alkanephosphonic Acids on Aluminum : Kinetics and Structure. *J. Phys. Chem. B* **2003**, *107*, 11726−11736.

https://doi.org/10.1021/acsomega.1c06183
ACS Omega 2022, 7, 1462−1467

(34) Shoute, L. C. T.; Hua, W.; Kisslinger, R.; Thakur, U. K.; Zeng, S.; Goswami, A.; Kumar, P.; Kar, P.; Shankar, K. Applied Surface Science Threshold Hydrophobicity for Inhibition of Salt Scale Formation on SAM- Modified Titania Nanotube Arrays. *Appl. Surf. Sci.* **2019**, *473*, 282−290.
(35) Hua, W.; Kar, P.; Roy, P.; Bu, L.; Shoute, L.; Kumar, P.; Shankar, K. Resistance of Superhydrophobic Surface-Functionalized TiO_2 Nanotubes to Corrosion and Intense Cavitation. *Nanomaterials* **2018**, *8*, 783.
(36) Chen, J.; Ruther, R. E.; Tan, Y.; Bishop, L. M.; Hamers, R. J. Molecular Adsorption on ZnO($10\bar{1}0$) Single-Crystal Surfaces: Morphology and Charge Transfer. *Langmuir* **2012**, *28*, 10437−10445.
(37) Paniagua, S. A.; Hotchkiss, P. J.; Jones, S. C.; Marder, S. R.; Mudalige, A.; Marrikar, F. S.; Pemberton, J. E.; Armstrong, N. R. Phosphonic Acid Modification of Indium-Tin Oxide Electrodes: Combined XPS/UPS/ Contact Angle Studies. *J. Phys. Chem. C* **2008**, *112*, 7809−7817.
(38) Chen, X.; Luais, E.; Darwish, N.; Ciampi, S.; Thordarson, P.; Gooding, J. J. Studies on the Effect of Solvents on Self-Assembled Monolayers Formed from Organophosphonic Acids on Indium Tin Oxide. *Langmuir* **2012**, *28*, 9487−9495.
(39) Modes, C. S.; Chains, A. C-H Stretching Modes and the Structure of n-Alkyl Chains. . Long, All-Trans Chains. *2J. Phys. Chem.* **1984**, *88*, 334−341.
(40) Spori, D. M.; Venkataraman, N. V.; Tosatti, S. G. P.; Durmaz, F.; Spencer, N. D.; Zürcher, S. Influence of Alkyl Chain Length on Phosphate Self-Assembled Monolayers. *Langmuir* **2007**, *23*, 8053−8060.
(41) Smecca, E.; Motta, A.; Fragalaì, M. E.; Aleeva, Y.; Condorelli, G. G. Spectroscopic and Theoretical Study of the Grafting Modes of Phosphonic Acids on ZnO Nanorods. *J. Phys. Chem. C* **2013**, *117*, 5364−5372.
(42) Quiñones, R.; Rodriguez, K.; Iuliucci, R. J. Investigation of Phosphonic Acid Surface Modi Fi Cations on Zinc Oxide Nanoparticles under Ambient Conditions. *Thin Solid Films* **2014**, *565*, 155−164.
(43) Tienes, B. M.; Perkins, R. J.; Shoemaker, R. K.; Dukovic, G. Layered Phosphonates in Colloidal Synthesis of Anisotropic ZnO Nanocrystals. *Chem. Mater.* **2013**, *25*, 4321−4329.
(44) National Astronomical Observatory of Japan. *Chronological Scientific Tables*; Maruzen: Tokyo, 2015.
(45) Kumbharkhane, A. C.; Puranik, S. M.; Mehrotra. Dielectric Relaxation of Tert-Butyl Alcohol-Water Mixtures Using a Time-Domain Technique. *J. Chem. Soc., Trans.* **1991**, *87*, 1569−1573.
(46) Pathan, A. W.; Kumbharkhane, A. C. Temperature-Dependent Relaxation Study of Tertiary Butyl Alcohol−Water Mixtures Using TDR Technique. *Phys. Chem. Liq.* **2017**, *55*, 179−185.
(47) Nakamura, K.; Takahashi, T.; Hosomi, T.; Seki, T.; Kanai, M.; Zhang, G.; Nagashima, K.; Shibata, N.; Yanagida, T. Redox-Inactive CO_2 Determines Atmospheric Stability of Electrical Properties of ZnO Nanowire Devices through a Roomerature Surface Reaction. *ACS Appl. Mater. Interfaces* **2019**, *11*, 40260−40266.
(48) Frisch, M. J.; Trucks, G. W.; Schlegel, H. B.; Scuseria, G. E.; Robb, M. a.; Cheeseman, J. R.; Scalmani, G.; Barone, V.; Petersson, G. a.; Nakatsuji, H.; Li, X.; Caricato, M.; Marenich, a. V.; Bloino, J.; Janesko, B. G.; Gomperts, R.; Mennucci, B.; Hratchian, H. P.; Ortiz, J. V.; Izmaylov, a. F.; Sonnenberg, J. L.; Williams; Ding, F.; Lipparini, F.; Egidi, F.; Goings, J.; Peng, B.; Petrone, A.; Henderson, T.; Ranasinghe, D.; Zakrzewski, V. G.; Gao, J.; Rega, N.; Zheng, G.; Liang, W.; Hada, M.; Ehara, M.; Toyota, K.; Fukuda, R.; Hasegawa, J.; Ishida, M.; Nakajima, T.; Honda, Y.; Kitao, O.; Nakai, H.; Vreven, T.; Throssell, K.; Montgomery, Jr., J. a.; Peralta, J. E.; Ogliaro, F.; Bearpark, M. J.; Heyd, J. J.; Brothers, E. N.; Kudin, K. N.; Staroverov, V. N.; Keith, T. a.; Kobayashi, R.; Normand, J.; Raghavachari, K.; Rendell, a. P.; Burant, J. C.; Iyengar, S. S.; Tomasi, J.; Cossi, M.; Millam, J. M.; Klene, M.; Adamo, C.; Cammi, R.; Ochterski, J. W.; Martin, R. L.; Morokuma, K.; Farkas, O.; Foresman, J. B.; Fox, D. J. G16_a03. 2016, p *Gaussian 16*, Revision A.03, Gaussian, Inc., Wallin.
(49) Johnson, R. D. Computational Chemistry Comparison and Benchmark Database, {NIST} Standard Reference Database 101. National Institute of Standards and Technology 2002.

https://doi.org/10.1021/acsomega.1c06183
ACS Omega 2022, 7, 1462−1467